Coexistence of superconductivity and magnetism in $K_xFe_{2-y}Se_{2-z}S_z$ ($z = 0,0.4$)

L. Li,[1,2] Z. R. Yang,[2,*] Z. T. Zhang,[1] W. Tong,[3] C. J. Zhang,[3] S. Tan,[1] and Y. H. Zhang[1,3]

[1]*High Magnetic Field Laboratory, University of Science and Technology of China, Hefei 230026, People's Republic of China*

[2]*Key Laboratory of Materials Physics, Institute of Solid State Physics, Chinese Academy of Sciences, Hefei 230031, People's Republic of China*

[3]*High Magnetic Field Laboratory, Hefei Institutes of Physical Science, Chinese Academy of Sciences, Hefei 230031, People's Republic of China*

(Received 28 January 2011; revised manuscript received 7 July 2011; published 4 November 2011)

Single crystals $K_xFe_{2-y}Se_{2-z}S_z$ ($z = 0$, 0.4) are successfully synthesized by self-flux method with the superconducting transition temperatures T_c^{onset} of 31.3 K and 32.8 K, respectively. In contrast to external pressure effect on superconductivity, the substitution of S for Se does not suppress T_c, which suggests that chemical doping may mainly modulate the anion height from the Fe layer rather than compressing interlayer distance. In electron spin resonance (ESR) measurements, a resonance signal arising from the paramagnetic (PM) Fe ions is detected at room temperature for both $K_xFe_{2-y}Se_2$ and $K_xFe_{2-y}Se_{1.6}S_{0.4}$ crystals. Upon cooling, the intensity of the spectrum weakens gradually and displays abrupt decrease below 140 K. The resonance signal disappears around 60 K ($\sim 2\ T_c$), corresponding to the saturation temperature of antiferromagnetic (AFM) order revealed by recent neutron-diffraction study. The evolution of ESR spectrum is discussed by correlating with recent neutron-diffraction and Raman-scattering results, in support of the coexistence of superconductivity and AFM order in $K_xFe_{2-y}Se_2$. Moreover, the variation of resonance field with decreasing temperature for $K_xFe_{2-y}Se_{1.6}S_{0.4}$ implies that the doping of S induces local weak ferromagnetism in the parent AFM background.

DOI: 10.1103/PhysRevB.84.174501 PACS number(s): 74.62.Fj, 74.70.−b

I. INTRODUCTION

During the past few years a lot of research efforts have been devoted to iron-based superconductors, mainly focusing on the interplay between superconductivity and magnetism.[1–12] The parent compounds of LnFeAsO (Ln is a rare-earth element),[1,2] $AeFe_2As_2$ (Ae is an alkali-earth element),[3,4] and iron chalcogenides FeSe(Te)[5–8] exhibit spin-density-wave (SDW) or antiferromagnetic (AFM) order. Chemical doping suppresses the magnetism, and superconductivity appears at a certain doping level.[9] In many cases the superconductivity is found to coexist with magnetism either in atomic scale or in nanoscale with electronic-phase separation characteristics.[8–10] These observations clearly indicate that the superconductivity in the iron-based superconductors is in proximity to magnetism, and spin fluctuation may play an important role for superconducting paring.[9] A direct correlation of superconductivity to spin fluctuation is the pressure effect on superconducting transition temperature T_c of FeSe.[11] T_c being dramatically increased to 37 K under high pressures is accompanied by the enhancement of spin fluctuation.[11] For higher pressures T_c decreases due to structure transition.[12] It is conjectured that if the structure transition under high pressure could be avoided, higher T_c could be expected in the iron chalcogenides.

Very recently, superconductivity with T_c around 30 K has been reported in FeSe-layered compound $A_xFe_{2-y}Se_2$ (A = K, Rb, Cs, Tl) with intercalating the alkaline metals between the FeSe layers.[13–18] The first-principles electronic structure calculations indicated that the ground state of AFe_2Se_2 is quasi-2-dimensional bicollinear or stripelike AFM with a magnetic moment of 2.8 or 2.26 μ_B around each Fe atom.[19,20] μSR, neutron-diffraction, Raman-scattering, and Mössbauer studies revealed that superconductivity in $K_xFe_{2-y}Se_2$ coexists with a strong AFM order with a large magnetic moment formed below an unprecedentedly high magnetic ordering temperature.[21–24] Nuclear magnetic resonance experiments showed weak ferromagnetic (FM) or AFM fluctuations in $K_xFe_{2-y}Se_2$.[25,26] Evolution from a superconducting state to an AFM-insulating state has been reported by varying Fe content.[18,27] These recent discoveries allow us to perform a direct comparison between FeSe(Te) and AFe_2Se_2. In the FeSe(Te) system the interplay between magnetism and superconductivity is mainly investigated by changing the ratio of anions.[7–10] First-principles calculations indicated that it is not the chalcogen species but rather the anion height from the Fe-plane that determines the magnetism.[28] Therefore the study of the anion-substitution effect on superconductivity in $A_xFe_2Se_2$ may shed light on the mechanism of unconventional superconductivity in this system.

In this paper we report the Se-site substitution effects on superconductivity and magnetism of $K_xFe_{2-y}Se_2$ system. The onset and zero-resistivity transition temperature of $K_xFe_{2-y}Se_{1.6}S_{0.4}$ were estimated to be 32.8 K and 31.2 K, respectively, slightly higher than those of the parent compound $K_xFe_{2-y}Se_2$. The electron spin resonance (ESR) studies performed on both $K_xFe_{2-y}Se_2$ and $K_xFe_{2-y}Se_{1.6}S_{0.4}$ show that the intensity of a paramagnetic (PM) resonance signal decreases gradually upon cooling below 300 K, and no evident resonance signal is observed with further decreasing temperature to 60 K. The evolution of the ESR signal is in exact comparison with more recent neutron and Raman-scattering studies, supporting for the coexistence of superconductivity and AFM order.[22,23] In addition the anion substitution-induced local weak ferromagnetism is revealed by the ESR spectra of $K_xFe_{2-y}Se_{1.6}S_{0.4}$.

II. EXPERIMENT

Single crystals of $K_xFe_{2-y}Se_{2-z}S_z$ ($z = 0, 0.4$) were grown using self-flux method. First, starting materials FeSe and

$FeSe_{0.8}S_{0.2}$ were prepared by reacting high-purity powder of iron, selenium, and sulfur at 650 °C for 12 hours. Then, the synthesized powder and K pieces were put into a small quartz tube with nominal compositions of $K_{0.8}Fe_2Se_2$ and $K_{0.8}Fe_2Se_{1.6}S_{0.4}$, respectively. The small quartz tube was sealed under high vacuum, put in a larger quartz tube, and was then followed by evacuating and being sealed. The mixture was heated up to 1050 °C and kept over 4 hours. Afterward the melt was cooled down to 700 ° C with the cooling rate 6 °C/h before the furnace was shut down.

The obtained crystals were characterized by powder x-ray diffraction (XRD) and x-ray single crystal diffraction with Cu K_α radiation at room temperature. Actual composition of the crystals was confirmed using energy dispersive x-ray (EDX) spectrometry. The resistivity was measured by using a standard four-probe method in a Quantum Design Physical Property Measurement System (PPMS). Magnetic properties were investigated using a superconducting quantum interference device (SQUID) magnetometer. ESR measurements were performed using a Bruker EMX plus 10/12 CW-spectrometer at X-band frequencies ($f \approx 9.36$ GHz) equipped with a continuous He gas-flow cryostat in the temperature region of 2–300 K by sweeping magnetic field parallel to the *ab*-plane and *c*-axis.

III. RESULTS AND DISCUSSION

Figure 1 shows the single crystal and powder XRD patterns for $K_xFe_{2-y}Se_{1.6}S_{0.4}$. For both components, only (*00l*) diffraction peaks appear in the single crystal XRD patterns, indicating that the *c*-axis is perpendicular to the cleavage surface. To examine the purity of the prepared crystals, we further performed powder XRD measurements by grinding several slides into powder for each component. All the peaks can be well indexed with the symmetry of $I4/mmm$, and no impurity phase is observed. The calculated-lattice parameters are $a = 3.9106$ Å, $c = 14.0663$ Å for $K_xFe_{2-y}Se_2$ and $a = 3.8560$ Å, $c = 14.0344$ Å for $K_xFe_{2-y}Se_{1.6}S_{0.4}$, similar to previously reported values.[13–15] Slight shrinkage of the lattice in

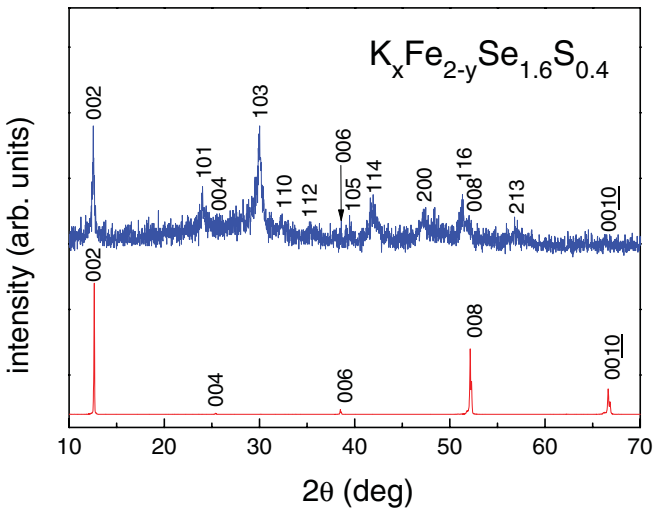

FIG. 1. (Color online) Powder XRD pattern and single crystal XRD pattern for $K_xFe_{2-y}Se_{1.6}S_{0.4}$.

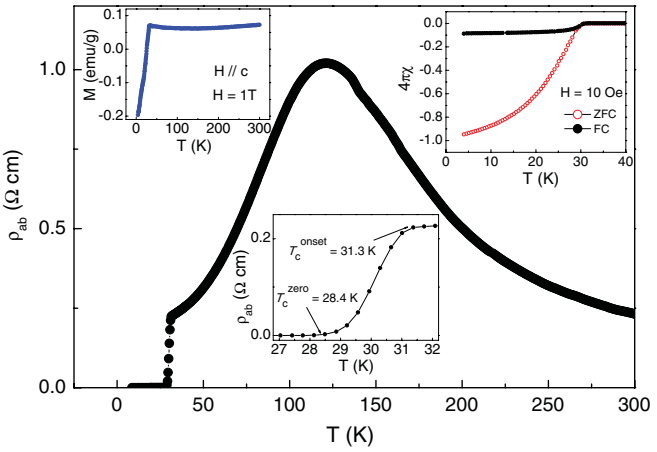

FIG. 2. (Color online) In-plane resistivity as a function of temperature for the parent compound $K_xFe_{2-y}Se_2$ crystal. The lower inset shows an enlarged view of superconducting transition from 27 K to 32 K. The ZFC and FC susceptibility taken at 10 Oe with the magnetic field parallel to the *ab*-plane is shown in the upper-right inset. The upper-left inset shows the magnetic susceptibility of $K_xFe_{2-y}Se_2$ with the magnetic field of 1 T applied parallel to the *c*-axis.

$K_xFe_{2-y}Se_{1.6}S_{0.4}$ indicates effective substitution of S for Se in the as-grown single crystals. The average stoichiometry of the as-grown samples was determined from EDX by examination of multiple points in the crystals. The measured compositions are $K_{0.79}Fe_{1.64(2)}Se_{2.00}$ and $K_{0.74}Fe_{1.67(5)}Se_{1.61}S_{0.40}$. We also measured the composition mapping using EDX. The results show that the spatial distribution of K, Fe, Se and S, is homogenous.

Figure 2 presents the in-plane resistivity and susceptibility results of the parent compound $K_xFe_{2-y}Se_2$. At high temperature, the resistivity increases with decreasing temperature and exhibits a broad hump at about 120 K. With further cooling, metallic transport behavior is observed, followed by superconducting transition at $T_c^{onset} \sim 31.3$ K. The abnormal hump in the resistivity curve has also been observed in $Rb_{0.8}Fe_2Se_2$ and $Cs_{0.8}Fe_2Se_2$, seemly to be a common feature in this system.[16,17,29] The temperature dependence of magnetic susceptibility with $H = 10$ Oe under both zero-field-cooling (ZFC) and field-cooling (FC) conditions is given in the upper-right inset of Fig. 2. It shows that the superconducting shield begins to emerge at about 30.4 K. The superconducting volume fraction estimated from the ZFC magnetization at 4 K is about 92%, which indicates the bulk superconductivity nature of the crystals. The upper-left inset shows the magnetic susceptibility of $K_xFe_{2-y}Se_2$ with the magnetic field of 1 T applied parallel to the *c*-axis. A sudden drop at about 30 K corresponds to the superconducting transition. The magnetic susceptibility weakly decreases with temperature below 300 K and exhibits a weak upturn below 140 K. The decrease in susceptibility with decreasing temperature at high temperatures has been correlated to the antiferromagnetism.[30,31]

The temperature dependence of resistivity for the $K_xFe_{2-y}Se_{1.6}S_{0.4}$ sample is shown in Fig. 3. The hump temperature $T_H \sim 131$ K is slightly higher than that in $K_xFe_{2-y}Se_2$. The lower inset of Fig. 3 shows the details of the superconducting transition; the onset and zero-resistivity

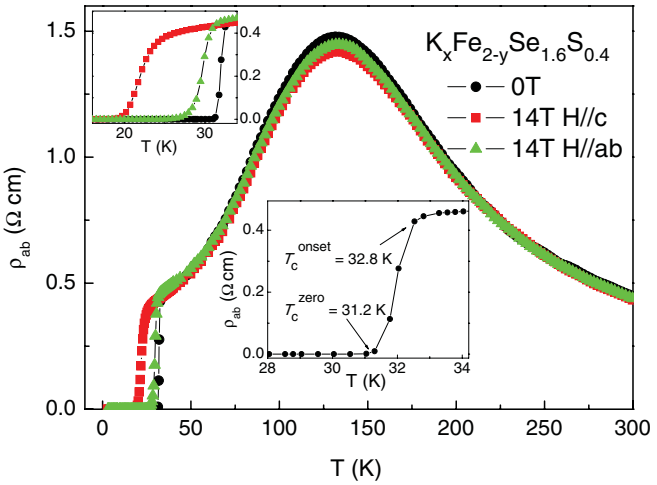

FIG. 3. (Color online) In-plane resistivity as a function of temperature for a $K_xFe_{2-y}Se_{1.6}S_{0.4}$ crystal with the magnetic fields of 0 T and 14 T parallel to the *c*-axis and the *ab*-plane, respectively. The lower inset shows an enlarged view of superconducting transition from 28 K to 34 K. The upper inset shows the zoom plot of resistivity around superconducting transition under external magnetic field.

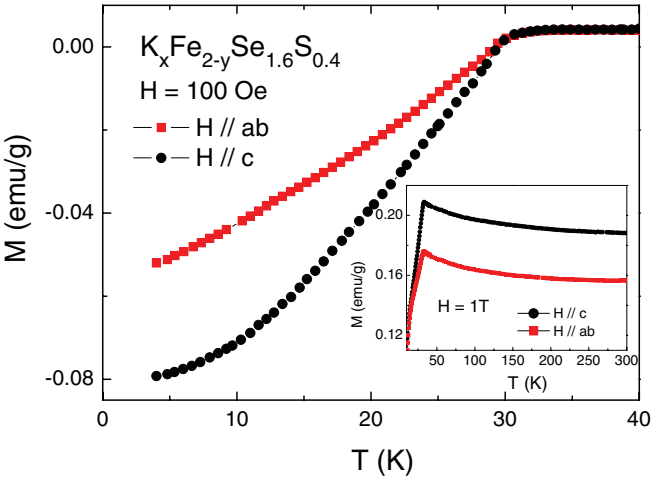

FIG. 4. (Color online) The magnetization at 100 Oe for single crystal $K_xFe_{2-y}Se_{1.6}S_{0.4}$ with the magnetic field parallel and perpendicular to *ab*-plane, respectively. The inset shows the magnetic susceptibility under a magnetic field of 1 T.

temperature were determined to be $T_c^{onset} = 32.8$ K and $T_c^{zero} = 31.2$ K, respectively. Both of them are slightly higher than those of the parent compound $K_xFe_{2-y}Se_2$, which is consistent with that reported by Lei *et al.*[32] Resistivity as a function of temperature under the magnetic field ($H = 14$ T) applied in *ab*-plane and along *c*-axis is also shown in Fig. 3. The transition temperature of superconductivity is suppressed, and the transition is broadened under external magnetic field; see the upper inset of Fig. 3. An obvious difference for the effect of field along a different direction on the superconductivity indicates the existence of anisotropy in $K_xFe_{2-y}Se_{1.6}S_{0.4}$ crystal. However, the hump peak in the resistivity curve has no obvious shift when applying magnetic field with no-matter *H*//*c*-axis or *H*//*ab*-plane.

Diamagnetism at low temperature in $K_xFe_{2-y}Se_{1.6}S_{0.4}$ can be clearly observed in magnetization measurements with magnetic field of 100 Oe, as seen in Fig. 4. The onset temperature T_c^{mag} of about 31 K is almost identical to the superconducting transition temperature T_c^{zero} in resistivity measurements. The inset of Fig. 4 shows magnetic susceptibility of $K_xFe_{2-y}Se_{1.6}S_{0.4}$ with the magnetic field of 1 T applied parallel to the *c*-axis and *ab*-plane from 10 K to 300 K. At low temperature, superconducting trace still exists, as revealed by the drop of susceptibility. Whether or not the external field is parallel to the *c*-axis, the magnetic susceptibility continually decreases with increasing the temperature from 33 K to 300 K, in disagreement with the case in parent compound $K_xFe_{2-y}Se_2$. The difference suggests that the magnetism is distinctly changed by the substitution of S for Se.

Since the ionic radius of S is smaller than that of Se, the substitution should produce positive chemical pressure. Recently, J. Guo *et al.* reported that both the T_c^{onset} and T_c^{zero} of $K_{0.8}Fe_{1.7}Se_2$ decreased with increasing pressure, and superconductivity disappeared under pressure above 9.2 GPa.[33] Similar suppression of superconductivity under external pressure was also found in $K_{0.85}Fe_2Se_{1.80}$ and $Cs_{0.86}Fe_{1.66}Se_2$.[34] However, Kawasaki *et al.* reported that T_c^{onset} increases with increasing pressure, while T_c^{zero} decreases.[35] In present work the doping with S does not decrease the transition temperature, implying that the effect of chemical pressure on superconductivity is different from that of external pressure. Considering AFe_2Se_2, the bond between the FeSe layers is via weak van der Waals force, which is fragile to external pressure. In contrast the substitution of S for Se may have more affect on modulating the bond between Fe and Se, thereby decreasing the anion height from the Fe layer. In FeTe(Se) the anion height is believed to play a key factor for determining the superconductivity and magnetism.[28]

We further performed ESR measurements to study the magnetism of the $K_xFe_{2-y}Se_2$ and $K_xFe_{2-y}Se_{1.6}S_{0.4}$ crystals, as shown in Figs. 5 and 6. The benefit of ESR is that it can give dynamic information of the local moment and magnetic correlation. In cuprate superconductors and their parent compounds ESR has been shown to be a highly sensitive tool to study the spin fluctuations and magnetic interactions. For the iron-based superconductors ESR experiments on $LaFeAsO_{1-x}F_x$ and $EuFe_2As_2$ have been carried out recently, which showed clear evidence for the existence of local moment and spin fluctuations.[36,37]

Figure 5 shows the ESR spectra of the $K_xFe_{2-y}Se_2$ sample from 2 K to 300 K for both *H*//*c*-axis and *H*//*ab*-plane. As the spectra signal at the temperature range of 40 K ∼ 300 K is very weak, we multiply the intensity in this temperature range by 10. The resonance field (H_{res}) is defined as the magnetic field corresponding to the midpoint between the highest and lowest points in the ESR spectrum. The effective *g* factor can be calculated with formula $g = (h\upsilon)/(\mu_B H_{res})$. At 300 K, there is a well-defined resonance signal located at about 0.32 T (with the *g* factor ∼ 2.083), which can be attributed to the local moment of PM-Fe ions, similar to the case of $LaFeAsO_{1-x}F_x$.[36] Upon cooling below 300 K, one can see that instead of increase, the intensity of the PM signal decreases for both the *H*//*c*-axis and *H*//*ab*-plane. We quantify the change of the resonance signal in the normal state between 40 K ∼

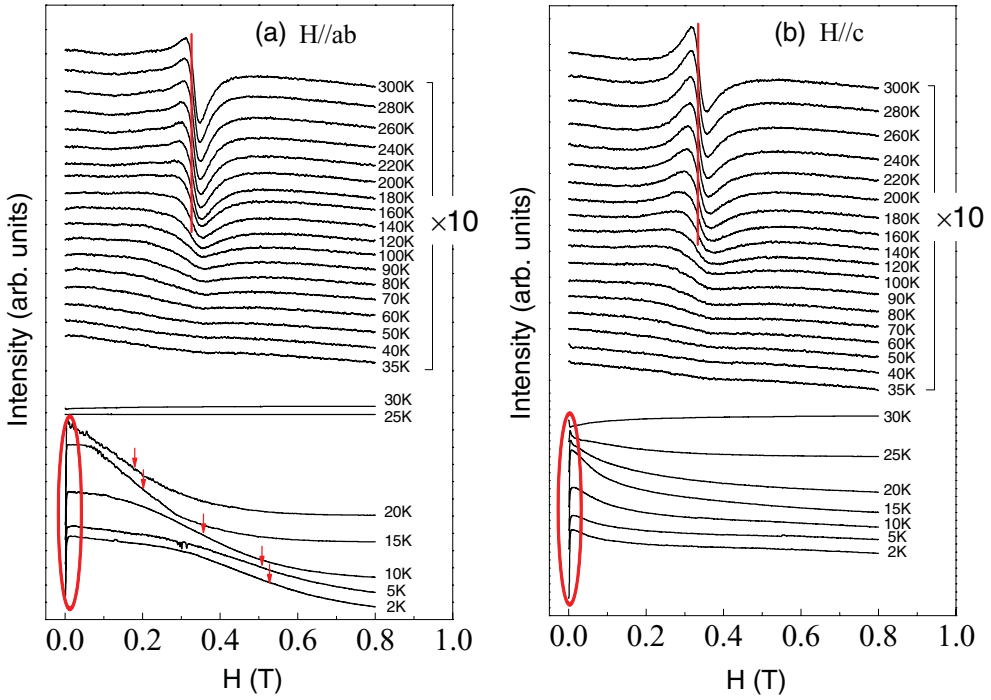

FIG. 5. (Color online) ESR spectra at different temperatures for $K_xFe_{2-y}Se_2$ crystal with sweeping magnetic field parallel to the *ab*-plane and *c*-axis, respectively. The intensity of the spectrum between 40 K and 300 K has been multiplied by 10. Red solid line denotes the resonance field. The superconducting-feature spectrum is marked by a red ellipse. Red arrow denotes the resonance field of the resonance-characteristic spectrum below T_c.

300 K by integrating the measured intensities, as shown in Fig. 7. The signal intensity drastically depresses below 140 K, and no evident resonance signal is observed at temperatures between 40 K and 60 K. With further decreasing temperature below 35 K, a diplike signal appears at low fields typical for the magnetic-shielding feature, indicating the appearance of superconductivity.

The temperature dependence of the ESR signal for the S-substituted sample $K_xFe_{2-y}Se_{1.6}S_{0.4}$ is given in Fig. 6. Similar to the case in $K_xFe_{2-y}Se_2$, one can see a PM signal at room temperature. With cooling temperature, the spectra intensity decreases gradually and disappears around 60 K. Both in Figs. 5(a) and 6(a), besides the diplike signal corresponding to superconductivity below 35 K, a novel resonance-characteristic spectrum appears and develops with further decreasing temperature, which is unexpected in conventional superconductors. Recently, Zhang *et al.* reported that the two-magnon Raman intensity in the superconducting state (9 K) would clearly lie below that in the normal state near T_c (35 K).[23] Moreover, the latest neutron-diffraction results from the group of W. Bao reveal that the magnetic-order parameter shows a sharp downturn as the temperature is lowered below T_c.[38] All of these results suggest that the superconductivity might be in proximity to magnetism in the $K_xFe_{2-y}Se_2$ system.

Since several less ambiguous techniques have revealed that superconductivity coexists with a large-moment AFM order in $K_{0.8}Fe_{1.6}Se_2$, it allows a direct comparison between ESR and other measurements.[21–24] In particular, neutron-diffraction investigation finds that in a wide temperature range below 500 K, the intensity of the (101) magnetic Bragg peak increases linearly with decreasing temperature and seems to saturate below $\sim 2T_c$ (around 60 K).[22] Comparing neutron scattering with ESR, the former is sensitive to AFM order but inert to PM, however ESR does the opposite because the AFM-resonance frequency is far from the X-band. From this point of view, ESR measurement can be regarded as a supplement for neutron scattering. In Fig. 7 one can see that instead of increase, the intensity of the PM signal decreases upon cooling below 300 K, signaling the decrease of PM-Fe ions. Those disappearing PM ions might develop into an AFM state and be responsible for the strengthening of AFM order, as revealed by neutron scatting.[22] It is interesting to note that upon further cooling, the PM-resonance signal disappears close to 60 K ($\sim 2\ T_c$), almost equaling the saturation temperature of AFM order in neutron-diffraction study.[22]

Besides similarities, different evolution of the ESR spectrum for two components is also observed. For $K_xFe_{2-y}Se_{1.6}S_{0.4}$, the PM signal not only weakens but also shifts to lower magnetic field upon cooling below 300 K for both $H//c$-axis and $H//ab$-plane. Moreover, a resonance signal at high field ($\sim$0.43 T) is detected when applying magnetic field along *c*-axis, as shown in Fig. 6(b). The changing of the resonance field gives direct evidence for the variation of magnetism upon doping S into $K_xFe_{2-y}Se_2$ in addition to the DC-susceptibility measurements.

In the ESR measurement the effective magnetic field $H_{\rm eff}$ experienced by the unpaired electrons can be written in simple form as $H_{\rm eff} = H_{\rm ext} + H_{\rm int}$. Here $H_{\rm ext}$ is the applied magnetic field, and $H_{\rm int}$ is the local internal magnetic field. For the case $H_{\rm int} > 0$, the internal field may cause the resonance line to shift to lower field; on the contrary, the resonance signal would appear at higher field with negative internal magnetic

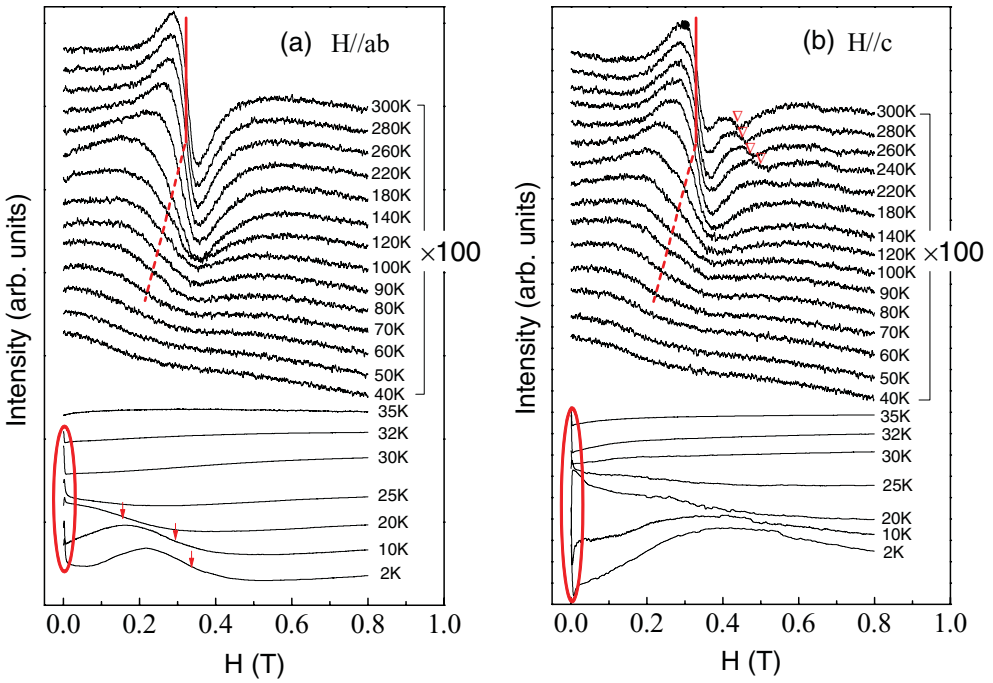

FIG. 6. (Color online) ESR spectra at different temperatures for $K_xFe_{2-y}Se_{1.6}S_{0.4}$ crystal with sweeping magnetic field parallel to the *ab*-plane and *c*-axis, respectively. The intensity of the spectrum between 35 K and 300 K has been multiplied by 100. Red solid and dashed lines denote the resonance field. Red triangle denotes an extra resonance signal at high field (∼0.43 T) with magnetic field parallel to *c*-axis at high temperatures between 240 K and 300 K. The superconducting-feature spectrum is marked by a red ellipse. Red arrow denotes the resonance field of the resonance characteristic spectrum below T_c.

field. Normally the resonance field, e.g., the *g* factor, should be temperature independent if the local internal field does not change as temperature. The strong temperature-dependent *g* factor caused by the change of internal magnetic field has also been observed in other iron-based superconductors. The change of internal magnetic field might arise from the magnetic fluctuation for $LaFeAsO_{1-x}F_x$[36] or might result from the homogenous polarization of the conduction electrons in the external field (Pauli susceptibility) for $EuFe_2As_2$.[37] Since there is no strong magnetic fluctuation in $K_xFe_{2-y}Se_2$[39] and

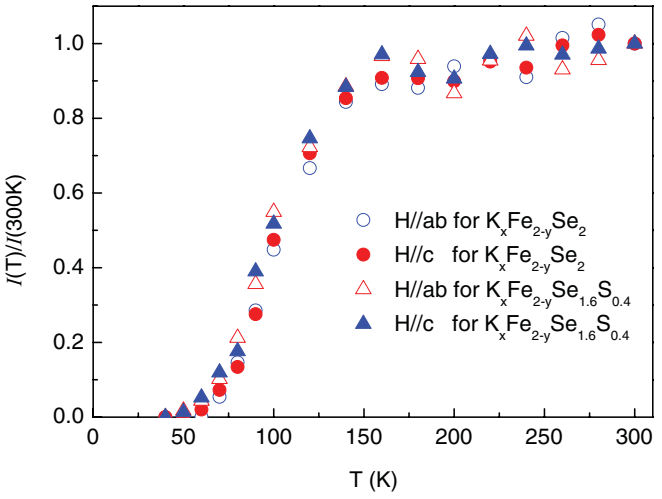

FIG. 7. (Color online) The temperature dependence of integrated resonance intensity in the normal state between 40 K ∼ 300 K for $K_xFe_{2-y}Se_2$ and $K_xFe_{2-y}Se_{1.6}S_{0.4}$.

the electronic-transport behavior does not change significantly with S substitution, the explanations by magnetic fluctuation or Pauli susceptibility could not be applied to $K_xFe_{2-y}Se_2$.

For $K_xFe_{2-y}Se_2$, in the ideal AFM background, the net internal magnetic field suffered by the PM-Fe ions is zero, therefore the *g* factor almost keeps constant with decreasing temperature. For $K_xFe_{2-y}Se_{1.6}S_{0.4}$, the resonance field depends on temperature on one hand, and extra resonance signal is detected at higher field when applying field along *c*-axis on the other hand. This indicates clearly that the substitution of S for Se changes the parent AFM background and induces local internal magnetic field. Early neutron-scattering experiment has revealed that the AFM order in $K_xFe_{2-y}Se_2$ is determined in an ordered vacancy structure with a $(\sqrt{5} \times \sqrt{5} \times 1)$ supercell.[22] The structure contains two iron sites; one is fully occupied (Fe1), while the other is almost completely empty (Fe2).[22,40] The magnetic structure is a "block checkerboard" structure with four Fe spins near the center of the unit cell pointing down, and four spins near the corners pointing up.[22] As reported in a similar iron chalcogenide system $FeTe_{1-x}Se_x$, doping Se into Te sites could transform the magnetic ordering from the $(\pi, 0)$ to the (π, π) by decreasing the Te-height from the Fe plane.[5,6,28] Analogously, replacing Se with S would also change the local environment of Fe-Se tetrahedral in $K_xFe_{2-y}Se_2$, as well as the occupation state in Fe1 and Fe2 sites. Therefore it is predictable that S-substitution may vary the exchange interactions between adjacent Fe ions and thereby induce local weak ferromagnetism into system. Consistent with our ESR results, recent study on $K_xFe_{2-y}Se_{2-z}S_z$ shows that the magnetism changes from AFM to spin glass upon doping

S on the Se site.[32] The local weak ferromagnetism can be the source of the internal magnetic field felt by the PM ions. The decrease of the resonance field with temperature implies the enhancement of the local ferromagnetism.

The high-field resonance signal in Fig. 6(b), which arises from the PM ions in negative internal magnetic fields, is absent in Fig. 6(a) for external field perpendicular to c-axis. Since the magnetic moments of Fe ions in the AFM state are oriented along the c-axis in $K_{0.8}Fe_{2-y}Se_2$,[22] the difference between the ESR spectra in Figs. 6(a) and 6(b) reveals the intrinsic anisotropy of the magnetism for $K_xFe_{2-y}Se_{1.6}S_{0.4}$. Nevertheless, to explore detailed evolution of the magnetic structure for $K_xFe_{2-y}Se_{1.6}S_{0.4}$, further studies by other techniques (e.g., neutron diffraction) are needed.

IV. CONCLUSION

In summary we have studied the Se-site substitution effects on superconductivity and magnetism in the $K_xFe_{2-y}Se_2$ system. Being contrary to external pressure effect, chemical pressure generated by the doping of S does not suppress T_c significantly. Detailed investigation on the evolution of ESR spectrum reveals that the PM component in system decreases with temperature and transforms into AFM phase entirely near 2 T_c. Sulfur substitution leads to the formation of weak ferromagnetism, which might be caused by the variation of the local Fe-Se tetrahedral structure and the decrease of the anion height from Fe-layer. The ESR results provide extra evidence for the coexistence of superconductivity with magnetism in addition to μSR, neutron-diffraction, Raman-scattering, and Mössbauer studies.

ACKNOWLEDGMENTS

This research was financially supported by the National Key Basic Research of China Grant Nos. 2007CB925001, 2010CB923403, and 2011CBA00111 and the National Nature Science Foundation of China Grant No. 11074258.

*Corresponding author: zryang@issp.ac.cn

[1] Y. Kamihara, T. Watanabe, M. Hirano, and H. Hosono, J. Am. Chem. Soc. **130**, 3296 (2008).
[2] Clarina de la Cruz, Q. Huang, J. W. Lynn, Jiying Li, W. Ratcliff II, J. L. Zarestky, H. A. Mook, G. F. Chen, J. L. Luo, N. L. Wang, and Pengcheng Dai, Nature (London) **453**, 899 (2008).
[3] Q. Huang, Y. Qiu, W. Bao, M. A. Green, J. W. Lynn, Y. C. Gasparovic, T. Wu, G. Wu, and X. H. Chen, Phys. Rev. Lett. **101**, 257003 (2008).
[4] J. H. Chu, J. G. Analytis, C. Kucharczyk, and I. R. Fisher, Phys. Rev. B **79**, 014506 (2009).
[5] S. L. Li, Clarina de la Cruz, Q. Huang, Y. Chen, J. W. Lynn, J. P. Hu, Y. L. Huang, F.-C. Hsu, K.-W. Yeh, Maw-Kuen Wu, and P. C. Dai, Phys. Rev. B **79**, 054503 (2009).
[6] W. Bao, Y. Qiu, Q. Huang, M. A. Green, P. Zajdel, M. R. Fitzsimmons, M. Zhernenkov, S. Chang, M. H. Fang, B. Qian, E. K. Vehstedt, J. H. Yang, H. M. Pham, L. Spinu, and Z. Q. Mao, Phys. Rev. Lett. **102**, 247001 (2009).
[7] T. J. Liu, J. Hu, B. Qian, D. Fobes, Z. Q. Mao, W. Bao, M. Reehuis, S. A. J. Kimber, K. Prokeš, S. Matas, D. N. Argyriou, A. Hiess, A. Rotaru, H. Pham, L. Spinu, Y. Qiu, V. Thampy, A. T. Savici, J. A. Rodriguez, and C. Broholm, Nat. Mater. **9**, 716 (2010).
[8] R. Khasanov, M. Bendele, A. Amato, P. Babkevich, A. T. Boothroyd, A. Cervellino, K. Conder, S. N. Gvasaliya, H. Keller, H.-H. Klauss, H. Luetkens, V. Pomjakushin, E. Pomjakushina, and B. Roessli, Phys. Rev. B **80**, 140511(R) (2009).
[9] M. D. Lumsden and A. D. Christianson, J. Phys. Condens. Matter **22**, 203203 (2010).
[10] L. Li, Z. R. Yang, Z. T. Zhang, L. Pi, S. Tan, and Y. H. Zhang, New J. Phys. **12**, 063019 (2010).
[11] T. Imai, K. Ahilan, F. L. Ning, T. M. McQueen, and R. J. Cava, Phys. Rev. Lett. **102**, 177005 (2009).
[12] S. Medvedev, T. M. McQueen, I. A. Troyan, T. Palasyuk, M. I. Eremets, R. J. Cava, S. Naghavi, F. Casper, V. Ksenofontov, G. Wortmann, and C. Felser, Nature Materials **8**, 630 (2009).
[13] J. G. Guo, S. F. Jin, G. Wang, S. C. Wang, K. X. Zhu, T. T. Zhou, M. He, and X. L. Chen, Phys. Rev. B **82**, 180520(R) (2010).
[14] A. Krzton-Maziopa, Z. Shermadini, E. Pomjakushina, V. Pomjakushin, M. Bendele, A. Amato, R. Khasanov, H. Luetkens, and K. Conder, J. Phys. Condens. Matter **23**, 052203 (2011).
[15] J. J. Ying, X. F. Wang, X. G. Luo, A. F. Wang, M. Zhang, Y. J. Yan, Z. J. Xiang, R. H. Liu, P. Cheng, G. J. Ye, and X. H. Chen, Phys. Rev. B **83**, 212502 (2011).
[16] A. F. Wang, J. J. Ying, Y. J. Yan, R. H. Liu, X. G. Luo, Z. Y. Li, X. F. Wang, M. Zhang, G. J. Ye, P. Cheng, Z. J. Xiang, and X. H. Chen, Phys. Rev. B **83**, 060512 (2011).
[17] C. H. Li, B. Shen, F. Han, X. Y. Zhu, and H. H. Wen, Phys. Rev. B **83**,184521 (2011).
[18] H. D. Wang, C. H. Dong, Z. J. Li, S. S. Zhu, Q. H. Mao, C. M. Feng, H. Q. Yuan, and M. H. Fang, Europhys. Lett. **94**, 27009 (2011).
[19] X.-W. Yan, M. Gao, Z.-Y. Lu, and T. Xiang, Phys. Rev. Lett. **106**, 087005 (2011).
[20] C. Cao and J. H. Dai, Chin. Phys. Lett. **28**, 057402 (2011).
[21] Z. Shermadini, A. Krzton-Maziopa, M. Bendele, R. Khasanov, H. Luetkens, K. Conder, E. Pomjakushina, S. Weyeneth, V. Pomjakushin, O. Bossen, and A. Amato, Phys. Rev. Lett. **106**, 117602 (2011).
[22] Wei Bao, Q. Huang, G. F. Chen, M. A. Green, D. M. Wang, J. B. He, X. Q. Wang, and Y. Qiu, Chin. Phys. Lett. **28**, 086104 (2011).
[23] A. M. Zhang, K. Liu, J. H. Xiao, J. B. He, D. M. Wang, G. F. Chen, B. Normand, Q. M. Zhang, e-print arXiv:1106.2706.
[24] D. H. Ryan, W. N. Rowan-Weetaluktuk, J. M. Cadogan, R. Hu, W. E. Straszheim, S. L. Bud'ko, and P. C. Canfield, Phys. Rev. B **83**, 104526 (2011).
[25] W. Yu, L. Ma, J. B. He, D. M. Wang, T.-L. Xia, G. F. Chen, and Wei Bao, Phys. Rev. Lett. **106**, 197001 (2011).
[26] H. Kotegawa, Y. Hara, H. Nohara, H. Tou, Y. Mizuguchi, H. Takeya, and Y. Takano, J. Phys. Soc. Jpn. **80**, 043708 (2011).
[27] D. M. Wang, J. B. He, T.-L. Xia, and G. F. Chen, Phys. Rev. B **83**, 132502 (2011).
[28] C.-Y. Moon and H. J. Choi, Phys. Rev. Lett. **104**, 057003 (2010).
[29] G. Seyfarth, D. Jaccard, P. Pedrazzini, A. Krzton-Maziopa, E. Pomjakushina, K. Conder, and Z. Shermadini, Solid State Commun. **151**, 747 (2011).

[30]H. C. Lei and C. Petrovic, Phys. Rev. B **83**, 184504 (2011).
[31]H. D. Wang, C. H. Dong, Z. J. Li, S. S. Zhu, Q. H. Mao, C. M. Feng, H. Q. Yuan, and M. H. Fang, Europhys. Lett. **93**, 47004 (2011).
[32]H. C. Lei, K. F. Wang, J. B. Warren, and C. Petrovic, e-print arXiv:1102.2434; Hechang Lei, M. Abeykoon, E. S. Bozin, and C. Petrovic, Phys. Rev. B **83**, 180503(R) (2011).
[33]J. Guo, L. L. Sun, C. Zhang, J. G. Guo, X. L. Chen, Q. Wu, D. C. Gu, P. W. Gao, X. Dai, and Z. X. Zhao, e-print arXiv:1101.0092.
[34]J. J. Ying, X. F. Wang, X. G. Luo, Z. Y. Li, Y. J. Yan, M. Zhang, A. F. Wang, P. Cheng, G. J. Ye, Z. J. Xiang, R. H. Liu, and X. H. Chen, New J. Phys. **13**, 033008 (2011).
[35]Y. Kawasaki, Y. Mizuguchi, K. Deguchi, T. Watanabe, T. Ozaki, S. Tsuda, T. Yamaguchi, H. Takeya, and Y. Takano, e-print arXiv:1101.0896.
[36]T. Wu, J. J. Ying, G. Wu, R. H. Liu, Y. He, H. Chen, X. F. Wang, Y. L. Xie, Y. J. Yan, and X. H. Chen, Phys. Rev. B **79**, 115121 (2009); J. J. Ying, T. Wu, Q. J. Zheng, Y. He, G. Wu, Q. J. Li, Y. J. Yan, Y. L. Xie, R. H. Liu, X. F. Wang, and X. H. Chen, *ibid.* **81**, 052503 (2010).
[37]E. Dengler, J. Deisenhofer, H.-A. Krug von Nidda, Seunghyun Khim, J. S. Kim, Kee Hoon Kim, F. Casper, C. Felser, and A. Loidl, Phys. Rev. B **81**, 024406 (2010); N. Pascher, J. Deisenhofer, H.-A. Krug von Nidda, M. Hemmida, H. S. Jeevan, P. Gegenwart, and A. Loidl, *ibid.* **82**, 054525 (2010).
[38]Mentioned by Q. M. Zhang *et al*., in Ref. 23.
[39]D. A. Torchetti, M. Fu, D. C. Christensen, K. J. Nelson, T. Imai, H. C. Lei, and C. Petrovic, Phys. Rev. B **83**, 104508 (2011).
[40]P. Zavalij, Wei Bao, X. F. Wang, J. J. Ying, X. H. Chen, D. M. Wang, J. B. He, X. Q. Wang, G. F. Chen, P.-Y. Hsieh, Q. Huang, and M. A. Green, Phys. Rev. B **83**, 132509 (2011).